Inorg. Chem. **2004**, *43*, 4944–4952

Density Functional Study of Ammonia Activation by Late First-Row Transition Metal Cations

Maria del Carmen Michelini, Nino Russo, and Emilia Sicilia*

Dipartimento di Chimica and Centro di Calcolo ad Alte Prestazioni per Elaborazioni Parallele e Distribuite-Centro d'Eccellenza MURST, Università della Calabria, I-87030 Arcavacata di Rende, Italy

Received March 9, 2004

Density functional theory (DFT) in its B3LYP implementation is used to investigate the reaction of ammonia with the late (Co^+, Ni^+, and Cu^+) first-row transition metal cations in both high- and low-spin states. The potential energy surfaces (PES's) leading to three different exit channels are closely examined. The binding energies for the reaction products are calculated and compared with the corresponding experimental values. A comparison with our earlier works covering the reactivity of the Sc–Fe series of cations is made in order to underline similarities and differences of the reaction mechanisms as well as to establish trends along the row.

1. Introduction

Over the past two decades, a great body of studies of gas-phase bimolecular reactions of bare transition metal cations with small molecules containing prototypical bonds (e.g., N−H, C−H, C−C, O−H) have been performed.[1−11] The interaction between metal ions and small ligands is experimentally studied by means of more or less sophisticated mass spectrometric techniques, which are able to provide thermochemical data as well as some insight into the reaction mechanisms. However, to obtain a deep knowledge of the reaction mechanisms as well as to unravel the origin of the observed reactivity trends, theoretical calculations are of fundamental importance.

From a theoretical point of view, first-row transition metals are extremely difficult to deal with, mainly because of the presence of unfilled valence d orbitals, which are characterized by their localization and high density of states. On the other side, a proper description of correlation effects, which play a crucial role in these systems, is mandatory.

The strong dependence of the reactivity and reaction pathways upon the metal cation electronic state is well-known. In this respect, the three late first-row metal cations (Co−Cu), unlike the rest of the elements of the row, all have low-spin ground states, whereas for the early and middle ones, i.e., from Sc to Fe, the lowest energy states are characterized by high-spin states. This fact undoubtedly determines the different behavior of these ions. Both experimental[12−14] and theoretical results[15] indicate that the interaction of early and middle single-charged transition metal ions with ammonia produces mainly the dehydrogenation product, MNH^+. It has been assumed that in the first stage of these reactions the reactants form a stable ion−dipole complex, MNH_3^+ (**I**). Then, the reaction proceeds via oxidative addition, i.e., insertion of M^+ into the N−H bond,

* Address correspondence to this author. E-mail: siliciae@unical.it. Phone: +39-0984-492048. Fax: +39-0984-492044.

(1) Allison, J.; Freas, R. B.; Ridge, D. P. *J. Am. Chem. Soc*. **1979**, *101*, 1332.
(2) *Gas-Phase Inorganic Chemistry*; Russel, D. H., Ed.; Plenum: New York, 1989; p 412.
(3) Armentrout, P. B.; Beauchamp, J. L. *Acc. Chem. Res.* **1993**, *26*, 213.
(4) Armentrout, P. B. In *Selective Hydrocarbons Activation: Principles and Progress*; Davies, J. A., Watson, P. L., Greenberg, A., Liebman, J. F., Eds.; VCH: New York, 1990.
(5) Armentrout, P. B. *Annu. Rev. Phys. Chem*. **1990**, *41*, 313.
(6) Eller, K.; Schwarz, H. *Chem. Rev.* **1991**, *91*, 1121.
(7) (a) Weisshaar, J. C. *Adv. Chem. Phys.* **1992**, 82, 213. (b) Weisshaar, J. C. *Acc. Chem. Res.* **1993**, *26*, 213.
(8) Armentrout, P. B.; Kickel, B. L. In *Organometallic Ion Chemistry*; Freiser, B. S., Ed.; Kluwer: Dordrecht, The Netherlands, 1996.
(9) Armentrout, P. B. In *Topics in Organometallic Chemistry*; Brown, J. M., Hofmann, P., Eds.; Springer-Verlag: Berlin, 1999.
(10) Crabtree, R. H. *The Organometallic Chemistry of the Transition Metals*, 2nd ed.; John Wiley & Sons: New York, 1994.
(11) Somorjai, G. A. *Introduction to Surface Chemistry and Catalysis*; John Wiley & Sons: New York, 1994.
(12) Clemmer, D. E.; Armentrout, P. B. *J. Phys. Chem*. **1991**, *95*, 3084 and references therein.
(13) Clemmer, D. E.; Sunderlin, L. S.; Armentrout, P. B. *J. Phys. Chem*. **1990**, *94*, 208.
(14) Clemmer, D. E.; Sunderlin, L. S.; Armentrout, P. B. *J. Phys. Chem*. **1990**, *94*, 3008.
(15) (a) Russo, N.; Sicilia, E. *J. Am. Chem. Soc*. **2001**, *123*, 2588. (b) Russo, N.; Sicilia, D. *J. Am. Chem. Soc*. **2002**, *124*, 1471. (c) Michelini, M. C.; Sicilia, E.; Russo, N. *J. Phys. Chem. A* **2002**, *106*, 8937. (d) Chiodo, S.; Kondakova, O.; Irigoras, A.; Michelini, M. C.; Russo, N.; Sicilia, E.; Ugalde, J. M. *J. Phys. Chem. A* **2004**, *108*, 1069.

10.1021/ic049696d CCC: $27.50
Published on Web 07/02/2004

to form the inserted intermediate $HMNH_2^+$ that may lie either lower or higher in energy than the reactants. Finally, from this hydrido-intermediate it is hypothesized that the reaction proceeds to yield a molecular hydrogen complex, $(H_2)M^+-NH$, after passing through a four-centered transition state. Dehydrogenation products are formed directly from this intermediate, and the reaction has been observed to be exothermic for early metals of the series. The other possible reaction products are MNH_2^+ and the metal hydride MH^+. In all the first-row transition metal cations, the products MNH_2^+ and MH^+ were observed in endothermic reactions.[13,14]

The reactivity of late first-row transition metal cations has been the subject of several earlier investigations. Indeed, some theoretical and experimental works have been carried out mainly concerning the reactivity of Co^+.[12,16−18] Despite this, a comparison of the different obtained results proves that the debate is open, and some unsolved questions still remain.

From the experimental point of view, the investigation of the interaction of Co^+ with ammonia[12,16] reveals that the dominant product at high energies is the metal hydride CoH^+, without large barriers in excess of the endothermicity. The formation of $CoNH_2^+$ dominates the reactivity over a brief energy range, whereas at the lowest kinetic energies the formation, exothermic and barrierless, of adduct ions is the only observed process. Unlike the reaction with early and middle first-row transition metals, no $CoNH^+$ formation is detected. Only the formation of the ion−dipole complex, $CoNH_3^+$, was found to be an exothermic process, and the authors have reported the formation of different structural isomers of the adduct, one of which was assigned to the intermediate structure $H-Co^+-NH_2$. Moreover, on the basis of the characteristics of the cross sections, it is suggested that CoH^+ and $CoNH_2^+$ formation occurs via direct reactions, without the involvement of a $H-Co^+-NH_2$ insertion intermediate.

On the theoretical side, Taketsugu and Gordon[17] have performed ab initio studies of the reaction mechanism of Co^+ with ammonia by applying complete active space self-consistent field (CASSCF), multireference configuration interaction (MR-SDCI), and multireference many-body perturbation theory (MRMP) levels of theory using both effective core potentials and all-electron methods. In this work, the relative energies of all the stationary points found along the potential energy surfaces (PES's) for both the triplet ground state and the quintet excited state were reported. The $H-Co^+-NH_2$ intermediate was predicted to be unstable in the case of the triplet spin state, whereas a quite stable minimum was found in the case of the quintet state. Almost at the same time, Vanquickenborne and co-workers[18] reported theoretical calculations by using CASSCF and CASPT2 techniques. In this case, only the reaction profile corresponding to the triplet spin state was reported. Even when the $H-Co^+-NH_2$ intermediate was confirmed as a stable structure, the authors proposed that this species does not actually work as an intermediate for the reaction between Co^+ and NH_3 because of the high energy barrier for the H_2 elimination. In consequence, it is hypothesized that the mechanistically simpler NH_2 and H eliminations proceed by simple Co−N and Co−H bond fission.

There have been only a small number of studies of the PES's in the case of the reactions of Ni^+ and Cu^+ with the ligand of interest. The interaction of these cations with NH_3 has been investigated by Hirao et al.[19] using multiconfigurational and multireference-based theories as well as by using the B3LYP approach of DFT. It is important to remark that only ground spin states, e.g., ^2D (d^9) in the case of Ni^+ and ^1S (d^{10}) for Cu^+, have been considered. The authors concluded that, in both cases, there exists no stable $H-M^+-NH_2$ intermediate complex. In consequence, they proposed that all the dissociations occur through highly vibrational excitations of the ion−dipole complex, MNH_3^+. From the experimental viewpoint, the previously cited work[12] of Clemmer and Armentrout also reports the results for the insertion of Ni^+ and Cu^+ cations into the N−H bond of ammonia. Analogous to the Co^+ cation, only the endothermic formation of MH^+ and MNH_2^+ products was observed at elevated energies, no MNH^+ species were detected, and at the lowest kinetic energies, the formation of the MNH_3^+ adduct was the only process observed to occur. The main difference with respect to the Co^+ reaction is the failure to detect a cross-sectional feature attributable to the insertion intermediates $HMNH_2^+$, explained by their lower stability. A study involving the interaction between first-row transition metal cations and ammonia[20] reports the sequential bond dissociation energies for the complex $M^+(NH_3)_x$ of the metal M = Ti−Cu. These data have been obtained by examining the collision-induced dissociation reactions with xenon in a guided ion beam mass spectrometer. Theoretical computations of the binding energy of the ion MNH_3^+ have been performed by Langhoff et al.[21] using the modified coupled-pair functional (MCPF) approach.

Because there exists an interest in understanding periodic trends of reactivity of the first-row transition metal cations with small ligands, the aim of the present contribution is to focus the attention on the comparison between the mechanisms of bond activation processes developed by late first-row transition metal cations with respect to earlier ones. To this end as well as to complement our prior systematic work[15] on this subject, we present a full description of reaction mechanisms for the interaction with ammonia of Co^+, Ni^+, and Cu^+ in both their high- and low-spin states. At the same time, we report the geometric and energetic properties of all the intermediates involved in the reaction pathways.

(16) Clemmer, D. E.; Armentrout, P. B. *J. Am. Chem. Soc*. **1989**, *111*, 8280.
(17) Taketsugu, T.; Gordon, M. S. *J. Chem. Phys.* **1997**, *106*, 8504.
(18) Hendrickx, M; Ceulemans, M.; Gong, K.; Vanquickenborne, L. *J. Phys. Chem*. *A* **1997**, *101*, 8540.
(19) Nakao, Y.; Taketsugu, T.; Hirao, K. *J. Chem. Phys.* **1999**, 110, 10863.
(20) Walter, D.; Armentrout, P. B. *J. Am. Chem. Soc*. **1998**, *120*, 3176.
(21) Langhoff, S. R.; Bauschlicher, C. W.; Partridge, H.; Sodupe, M. *J. Phys. Chem*. **1991**, *95*, 10677.

2. Computational Details

The density functional theory (DFT) in its three-parameter hybrid B3LYP[22,23] formulation was the computational method used for geometry optimization and frequency calculations together with the DZVP[24] (for the transition metal) and TZVP[25] (for the other atoms) basis sets.

The results of several theoretical works performed in recent years clearly show that the B3LYP approach in conjunction with the DZVP and TZVP basis sets can be confidently used to obtain reliable results for the systems of interest in this work.[15,26] Moreover, as the result of our previous works on this subject, we have concluded that the methodology of performing geometry optimizations at the B3LYP/DZVP level of theory, followed by single point calculations using the TZVP+G(3df,2p) basis set[26] for the metal, allows us to obtain accurate results. No symmetry restrictions have been imposed, whereas for each optimized stationary point, vibrational analysis was carried out to determine its character (minimum or saddle point) and to evaluate the zero-point vibrational energy (ZPE) corrections, which are included in all relative energies. For transition states, it was carefully checked that the vibrational mode associated with the imaginary frequency corresponded to the correct movement of involved atoms. Basis set superposition errors (BSSEs) have been calculated by using the counterpoise method.[27] For all the studied species, we have checked $\langle S^2 \rangle$ values to evaluate if spin contamination can influence the quality of the results. In all cases, we have found that the calculated values differ from $S(S+1)$ by less than 10%. For the sake of brevity, the B3LYP/TZVP+G(3df,2p)//B3LYP/DZVP computations will be referred to as B3LYP/TZVP.

All the calculations reported in this work have been carried out with the GAUSSIAN98/DFT[28] code.

We present, in addition, a topological description of all the key minima and transition states found along the PES's with the aim of investigating the nature of the bonding. In particular, we have used the topological analysis of the electron localization function (ELF) as proposed by Silvi and Savin.[29] The fundamentals[29,30] and applications of this method to the understanding of the chemical bond[31,32] and reactivity in terms of elementary catastrophes[33−35] are well documented. Recent work[15d,36−38] demonstrates that this method is a reliable tool to analyze the nature of the chemical bonds present in systems involving transition metals.

ELF calculations have been carried out with the TopMod package developed at the Laboratoire de Chimie Théorique de l'Université Pierre et Marie Curie.[39,40] Graphical representations of the bonding are obtained by plotting isosurfaces of the localization functions using the public domain scientific visualization and animation program for high-performance graphic workstations named SciAn.[41]

Table 1. Relative Energies, in kcal/mol, of the M^+ Excited State with Respect to Ground State

cation	configurations (state)	B3LYP/DZVP[a]	B3LYP/TZVP[a]	expt[b]
Co^+	d^8 (^{3}F)−sd^7 (^{5}F)	21.6	16.7	9.9
Ni^+	d^9 (^{2}D)−sd^8 (^{4}F)	31.9	28.0	25.0
Cu^+	d^{10} (^{1}S)−sd^9 (^{3}D)	69.1	67.1	64.8

[a] Reference 26. [b] Reference 42.

3. Results and Discussion

3.1. Excitation Energies. It is well-known that a correct prediction of the interconfigurational energy ordering of the two valence electronic configurations, sd^{n-1} and d^n, of transition metal ions is fundamental in order to ensure a proper description of the entire reaction pathways. Because of this, we first briefly analyze the calculated splitting between the ground and excited states of interest for the bare cations. The relative energies of the M^+ excited states with respect to the ground state are summarized in Table 1.

The B3LYP/DZVP and B3LYP/TZVP calculations already reported[26] give for the three examined cations the following results. The ^{3}F (d^8) was found as the ground state of Co^+, with the low-lying ^{5}F (sd^7) excited state lying 21.6 and 16.7 kcal/mol higher in energy at B3LYP/DZVP and B3LYP/TZVP levels of theory, respectively. These results overestimate the experimental gaps[42] of 11.7 and 6.8 kcal/mol, respectively.

In the case of Ni^+ and Cu^+, results are more accurate and in qualitative agreement with the corresponding experimental data.[42] For Ni^+, a ^{2}D (d^9) ground state followed by an ^{4}F (sd^8) state is found 31.9 and 28.0 kcal/mol above at B3LYP/DZVP and B3LYP/TZVP levels of theory, respectively. The Cu^+ electronic ground state corresponds to an ^{1}S (d^{10}) state, with the ^{3}D (sd^9) state lying 69.1 and 67.1 kcal/mol above at the respective levels of theory. In this case, the overestimation of the experimental value is only 4.3 and 2.3 kcal/mol, respectively.

In summary, even when the B3LYP approximation correctly predicts in all cases the energetic ordering for all three cations, the energy gaps are overestimated in all cases, this difference being particularly marked in the case of Co^+.

(22) Becke, A. D. *J. Chem. Phys.* **1993**, *98*, 5648.
(23) Stephens P. J.; Devlin, F. J.; Chabalowski, C. F.; Frisch, M. J. *J. Phys. Chem.* **1994**, *98*, 11623.
(24) Andzelm, J.; Radzio, E.; Salahub, D. R. *J. Comput. Chem.* **1985**, *6*, 520.
(25) Goudbout, N.; Salahub, D. R.; Andzelm, J.; Wimmer, E. *Can. J. Chem.* **1992**, *70*, 560.
(26) Irigoras, A.; Elizalde, O.; Silanes, I.; Fowler, J. E.; Ugalde, J. M. *J. Am. Chem. Soc.* **1989**, *111*, 8280 and references herein.
(27) Boys, S. B.; Bernardi, F. *Mol. Phys.* **1970**, *19*, 553.
(28) Frisch, M. J.; Trucks, G. W.; Schlegel, H. B.; Gill, P. M. W.; Johnson, B. G.; Robb, M. A.; Cheeseman, J. R.; Keith, T.; Petersson, G. A.; Montgomery, J. A.; Raghavachari, K.; Al-Laham, M. A.; Zakrzewski, V. G.; Ortiz, J. V.; Foresman, J. B.; Cioslowski, J.; Stefanov, B. B.; Nanayakkara, A.; Challacombe, M.; Peng, C. Y.; Ayala, P. Y.; Chen, W.; Wong, M. W.; Andres, J. L.; Replogle, E. S.; Gomperts, R.; Martin, R. L.; Fox, D. J.; Binkley, J. S.; Defrees, D. J.; Baker, J.; Stewart, J. P.; Head-Gordon, M.; Gonzalez, C.; Pople, J. A. *Gaussian 94*, revision A.1; Gaussian, Inc.: Pittsburgh, PA, 1995.
(29) Silvi, B.; Savin, A. *Nature* **1994**, *371*, 683.
(30) Becke, A. D.; Edgecombe, K. E. *J. Chem. Phys.* **1990**, *92*, 5397.
(31) Savin, A.; Nesper, R.; Wengert, S.; Fässler, T. F. *Angew. Chem., Int. Ed. Engl.* **1997**, *36*, 1809.
(32) Noury, S.; Silvi, B.; Gillespie, R. G. *Inorg. Chem.* **2002**, *41*, 2164.
(33) Krokidis, X.; Noury, S.; Silvi, B. *J. Phys. Chem. A* **1997**, *101*, 7277.
(34) Krokidis, X.; Vuilleumier, R.; Borgis, D.; Silvi, B. *Mol. Phys.* **1999**, *96*, 265.
(35) Krokidis, X.; Moriarty, N. W.; Lester, W. A., Jr.; Frenklach, M. *Chem. Phys. Lett.* **1999**, *314*, 534.
(36) Michelini, M. C.; Sicilia, E.; Russo, N.; Alikhani, M. E.; Silvi, B. *J. Phys. Chem. A* **2003**, *107*, 4862.
(37) Pilme, J.; Silvi, B.; Alikhani, M. E. *J. Phys. Chem. A* **2003**, *107*, 4506.
(38) Michelini, M. C.; Sicilia, E.; Russo, N. *Inorg. Chem.* **2003**, *42*, 8773.
(39) Noury, S.; Krokidis, X.; Fuster, F.; Silvi, B. *TopMod Package*; Paris, 1997.
(40) Noury, S.; Krokidis, X.; Fuster, F.; Silvi, B. *Comput. Chem. (Oxford)* **1999**, *23*, 597.
(41) Pepke, E.; Muray, J.; Lyons, J. *Scian*; Supercomputer Computations Research Institute, Florida State University: Tallahassee, FL, 1993.
(42) Moore, C. E. *Atomic Energy Levels*; NSRD-NBS, U.S.A.; U.S. Government Printing Office: Washington, DC, 1991; Vol. 1.

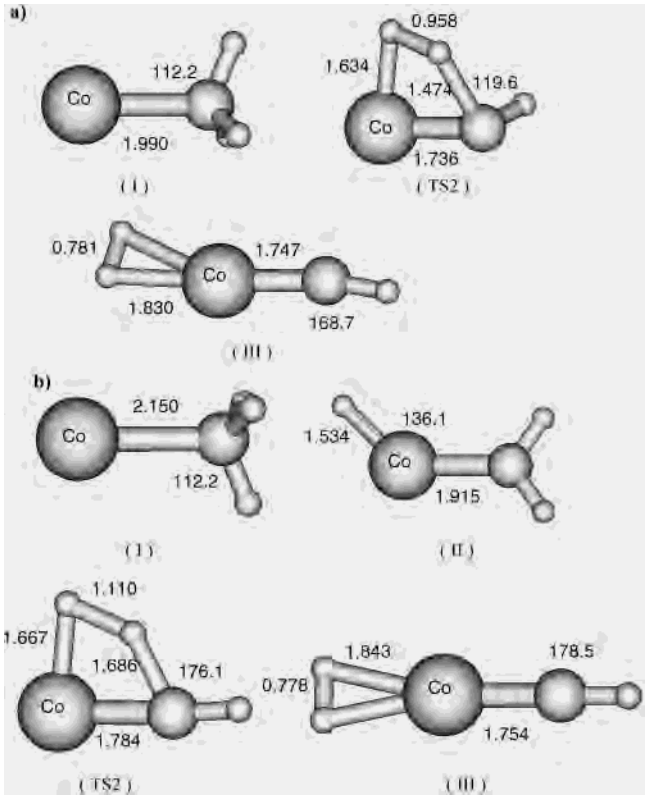

Figure 1. Geometric parameters of minima and transition states on the B3LYP/DZVP (a) triplet and (b) quintet PES's for the reaction of Co^+ with NH_3. Bond lengths are in angstroms and angles in degrees.

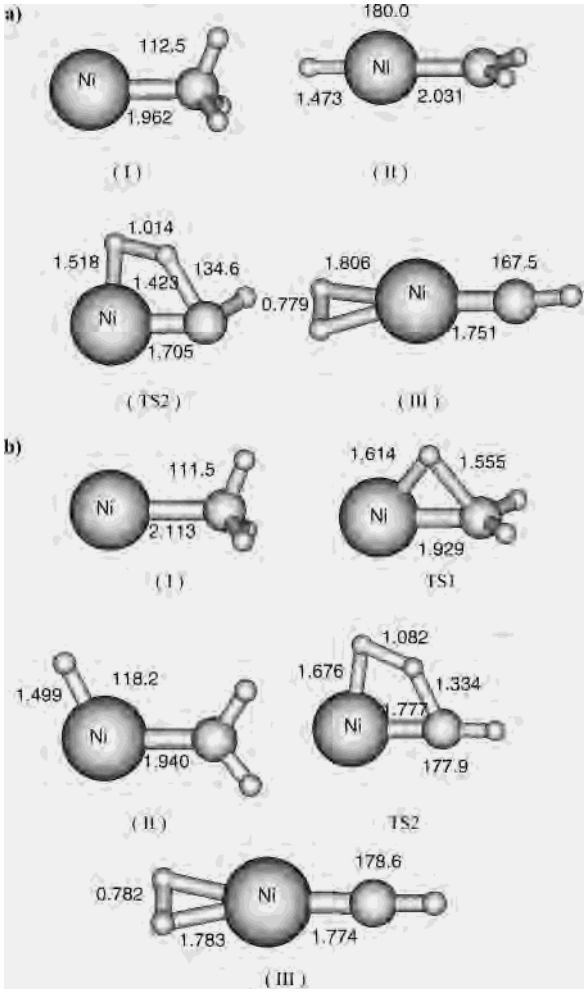

Figure 2. Geometric parameters of minima and transition states on the B3LYP/DZVP (a) doublet and (b) quartet PES's for the reaction of Ni^+ with NH_3. Bond lengths are in angstroms and angles in degrees.

3.2. Activation Reaction Mechanisms. Geometric parameters of stationary points found along the pathways, for both the triplet and quintet states of Co^+, are reported in Figure 1a,b, respectively. The corresponding parameters for the doublet and quartet spin states of Ni^+ and the singlet and triplet spin states of Cu^+ are shown in Figures 2a,b and 3a,b, respectively. The potential energy profiles are sketched in Figure 4, which shows the relative energies of all the intermediates, transition states, and exit channels with respect to the ground state asymptotes.

The first step of the reaction is the exothermic formation of the ion−molecule complex (**I**) at both the low- and high-spin states. For the ground states, the stabilization energy is quite similar for all three metals. As can be seen in Table 2, both levels of theory, B3LYP/DZVP and B3LYP/TZVP, succeed at reproducing experimental binding energies to a very good extent. Other previously calculated values are collected in the same table with the aim of comparison, showing the very good performance of our adopted computational protocol. Even though the low-spin adduct formation has been found to be the only exothermic step along the path for the final hydrogen elimination (see Figure 4), all the species that are expected in a dehydrogenation process of ammonia, according to the findings for early and middle transition metals, have been analyzed. The hypothesized $H-M^+-NH_2$ insertion intermediate (**II**), whose existence has been considered controversial by other authors, has been found to be a stable species for both high- and low-spin states for all three considered cations. In all cases, the high-spin state is lower in energy, in contrast with a prediction of a more stable low-spin intermediate due to the formation of two covalent σ bonds. An electrostatic interaction between the cation, bonded to the H atom, and the NH_2 moiety stabilizes the high-spin complexes with respect to the low-spin ones. For all three metal ions, the energy difference between the high- and low-spin states decreases progressively from Co^+ to Ni^+ to Cu^+. Indeed, for $H-Cu^+-NH_2$, the assignment of the ground state is tenuous. Very good agreement exists between the values, theoretically calculated and estimated using experimental data, of the energy formation of intermediate (**II**) from reactants (Table 2).

The $HMNH_2^+$ insertion intermediate formation would occur through a transition state corresponding to the shift of a hydrogen atom from the nitrogen atom to the metal center. Structures and energies of such maxima are well established for the high-spin states of all the examined cations, whereas all the attempts to localize them along the low-spin energy paths were unsuccessful. Although this failure prevents us from characterizing the crossing region between the surfaces, in any case, the very high barrier to formation of intermediate (**II**) hinders the formation of this precursor of dehydrogenation products. The calculated value of ~25 kcal/mol for

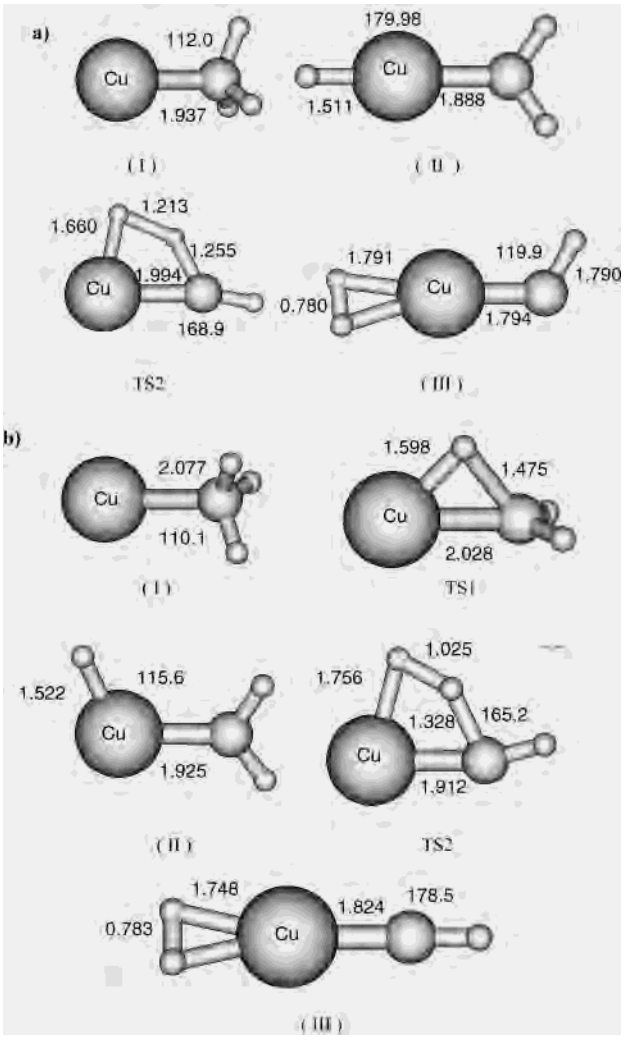

Figure 3. Geometric parameters of minima and transition states on the B3LYP/DZVP (a) singlet and (b) triplet PES's for the reaction of Cu^+ with NH_3. Bond lengths are in angstroms and angles in degrees.

the barrier with respect to the entrance channel along the path for the Co^+ cation agrees well with the value of 20 kcal/mol suggested by Clemmer et al. A barrier of 18 kcal/mol was proposed by them for the reverse reaction (i.e., from the insertion to initial ion−dipole complex), and ∼20 kcal/mol is the value calculated by us. Barriers that are considerably higher have been calculated for the insertion step of the other two cations.

After $HMNH_2^+$ insertion intermediate formation, the reaction proceeds to yield the molecular hydrogen complex, $(H_2)MNH^+$ (**III**), overcoming a TS2 four-centered transition state. In all three reaction pathways, the high- and low-spin state TS2 structures were located very close in energy; in particular, in the case of Co^+, the minima are almost degenerate (within 1 kcal/mol). Finally, the dehydrogenation products, MNH^+, could be formed directly from (**III**) without an energy barrier.

Results concerning the other possible exit channels, i.e., formation of MNH_2^+ and MH^+ products, can be summarized as follows. The endothermicities of the reactions for the formation of MNH_2^+ species are very close to those of the dehydrogenation process. For Co^+, this difference is ∼3.5

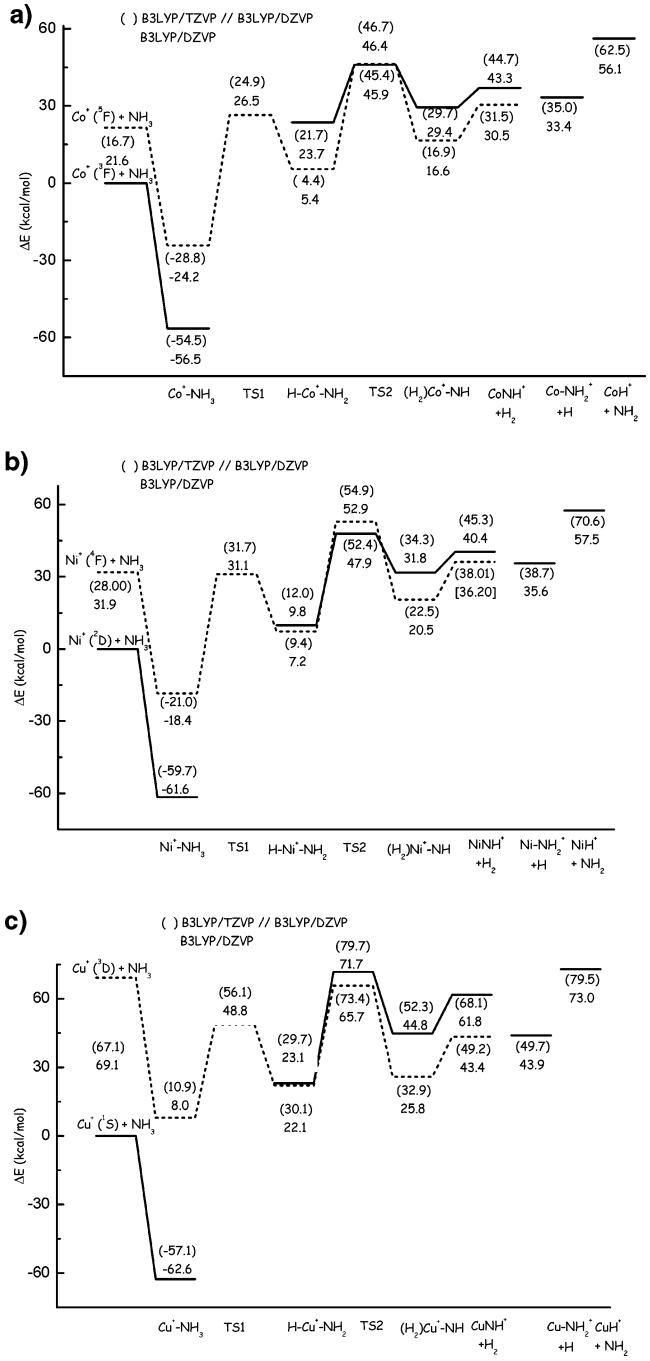

Figure 4. B3LYP/DZVP PES's for the reaction with NH_3 of (a) triplet and quintet Co^+, (b) doublet and quartet Ni^+, and (c) singlet and triplet Cu^+. B3LYP/TZVP relative energies are in parentheses. Energies are in kcal/mol and relative to the ground-state reactants.

kcal/mol and is not significant for the other two cations. At the same time, the elimination of the MNH_2^+ fragment is thermodynamically favored with respect to MH^+ formation. Reaction energies calculated by us for these processes are significantly lower than those estimated using thermochemical data[20] (see Table 2).

From these results, the picture which can be drawn is in very good agreement with the ideas previously presented to explain why no MNH^+ products were observed for the late first-row transition metals. At low kinetic energies, only the formation of the initial ion−molecule complex is possible.

Table 2. Relative Energies, in kcal/mol, of M^+-NH_3 (ΔE), HM^+-NH_2 (ΔE_1), $MNH_2^+ + H$ (ΔE_2), $MNH^+ + H_2$ (ΔE_3), and $MH^+ + NH_2$ (ΔE_4) Products with Respect to the Ground State of Reactants[a]

system	method	ΔE	ΔE_1	ΔE_2	ΔE_3	ΔE_4
$Co^+(^5F) + NH_3$	B3LYP/TZVP[b]	−53.0(1.4)	4.4	35.0	31.5	62.5
	B3LYP/DZVP[b]	−53.1(3.4)	5.4	33.4	30.5	56.1
	MR−SDCI[c]	−52.1	−3.3	46.2		55.2
	CASSCF[c]	−44.1	4.9	56.7		56.3
	CASPT2[d]	−52.1	−6.5	34.2	21.7	50.6
	MCPF[e]	−53.2				
	expt	-55.1 ± 3.8[f]	∼0.0[g]	46.0 ± 1.6[g]		65.5 ± 1.4[g]
$Ni^+(^4F) + NH_3$	B3LYP/TZVP[b]	−58.2(1.5)	9.4	38.7	38.0	70.6
	B3LYP/DZVP[b]	−57.6(4.0)	7.2	35.6	36.2	57.5
	SA-CASSCF[h]	−51.7	−18.9	34.7	34.0	23.1
	MR−SDCI[h]	−50.9	11.8	53.6	55.0	59.6
	B3LYP[h]	−59.0	6.0	43.5	45.3	62.8
	MCPF[e]	−57.5				
	expt	-58.2 ± 4.5[f]	∼13.8[g]	52.6 ± 1.8[g]		68.5 ± 1.8[g]
$Cu^+(^1S) + NH_3$	B3LYP/TZVP[b]	−55.8(1.3)	29.7	49.7	49.2	79.5
	B3LYP/DZVP[b]	−58.0(4.5)	23.1	43.9	43.4	73.0
	SA-CASSCF[h]	−47.8	12.0	40.1	77.1	62.1
	MR−SDCI[h]	−48.1	41.6	56.5	90.1	92.2
	B3LYP[h]	−57.8	22.1	49.1	89.8	72.3
	MCPF[e]	−54.7				
	expt	-59.7 ± 3.6[f]	∼36.9[g]	60.0 ± 3.0[g]		86.0 ± 3.0[g]

[a] Ground states of products are as follows: Co^+-NH_3 ($^3A_2$), $H-Co^+-NH_2$ ($^5A'$), $CoNH_2^+$ ($^4A_1$), $CoNH^+$ ($^5\Delta$), CoH^+ ($^4\Phi$), Ni^+-NH_3 ($^2A_1$), $H-Ni^+-NH_2$ ($^4A'$), $NiNH_2^+$ ($^3A'$), $NiNH^+$ ($^4A''$), NiH^+ ($^3\Delta$), Cu^+-NH_3 ($^1A_1$), $H-Cu^+-NH_2$ ($^3A'$), $CuNH_2^+$ ($^2A_1$), $CuNH^+$ ($^3A''$), and CuH^+ ($^2\Sigma^+$). BSSEs are reported in parentheses. [b] The basis sets refer to the metal atom. [c] Ref 17. [d] Ref 18. [e] Ref 21. [f] Ref 20. [g] Ref 12. [h] Ref 19.

Table 3. Binding Energies of the Ground State Reaction Products Corresponding to the Ammonia Reaction[a]

level of theory	CoH^+	$CoNH_2^+$	$CoNH^+$	NiH^+	$NiNH_2^+$	$NiNH^+$	CuH^+	$CuNH_2^+$	$CuNH^+$
B3LYP/DZVP[b]	46.5(1.5)	55.4(3.5)	57.6(3.3)	45.0(1.7)	53.3(3.4)	51.4(3.8)	29.1(2.0)	44.6(3.7)	43.9(4.0)
B3LYP/TZVP[b]	40.6(1.0)	55.8(1.5)	58.7(1.2)	42.5(1.0)	52.8(0.8)	52.2(1.2)	23.6(1.1)	41.7(0.8)	41.0(1.2)
expt[c]	46.7 ± 1.4	59.0 ± 1.6		39.7 ± 1.8	53.3 ± 1.8		22.1 ± 3.0	45.9 ± 3.0	

[a] BSSE corrections are reported in parentheses. All the values are in kcal/mol. [b] The basis sets refer to the metal atom. [c] Ref 12.

At higher energies, the insertion intermediate also becomes accessible, but because of the high energy barriers that hamper their formation, the direct production of MNH_2^+ and MH^+ moieties from TS1 by simple metal−nitrogen and metal−hydrogen bond cleavage is more likely to occur. Even when the formation of the $HMNH_2^+$ intermediate is considered possible, as in the case of Co^+ ion, the dehydrogenation process, which involves a tight transition state, cannot be competitive.

To strengthen the quantitative reliability of the examined PES's, we have collected in Table 3 the bond dissociation energies for all the fragments formed as a result of the interaction of the ammonia molecule with Co^+, Ni^+, and Cu^+ cations and compared them with experimental data,[12] when available.

3.3. ELF Analysis. The localization domains of all the species involved in the reaction of Co^+ with ammonia are displayed in Figure 5. For the rest of the metals, the topological characteristics of every minimum are analogous to the corresponding ones for Co^+; therefore, we will present a general description for all three reactions (M = Co, Ni, Cu). In Figure 5, we include the topological description of the first minimum (**I**) for both low-spin (a) and high-spin (b) states, whereas the rest of the figure corresponds to the lowest-energy high-spin states. It can be seen that for the initial complex (**I**) the main topological difference between the isomers consists of the presence of a monosynaptic valence basin, V(M), in the high-spin isomer (see Figure 5a, part I), which is absent for the low-spin state. This fact can be understood by considering the electronic configuration that characterizes the low-spin metal states (d^n) and taking into account that within ELF analysis the electron density

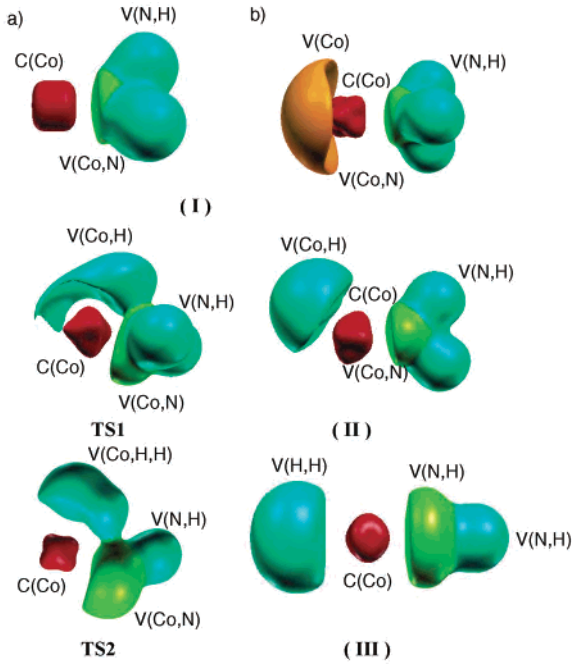

Figure 5. ELF localization domains for all the key minima involved in the reaction paths of Co^+ with ammonia. The bounding isosurfaces are ELF = 0.60.

Table 4. Equilibrium Geometry Parameters for Ground-State Products at the B3LYP/DZVP Level of Theory[a]

product (state)	M−N	M−H	N−H	M−N−H	M−N−H−H
CoH^+ ($^4\Phi$)		1.551			
$CoNH^+$ ($^5\Delta$)	1.738		1.024	180.0	
$CoNH_2^+$ ($^4A_1$)	1.786		1.019	125.1	179.9
NiH^+ ($^3\Delta$)		1.541			
$NiNH^+$ ($^4A''$)	1.746		1.023	172.9	
$NiNH_2^+$ ($^3A'$)	1.783		1.023	124.7	179.4
CuH^+ ($^2\Sigma^+$)		1.487			
$CuNH^+$ ($^3A''$)	1.800		1.028	167.1	
$CuNH_2^+$ ($^2A_1$)	1.838		1.023	125.0	179.1

[a] Bond lengths are in Å and angles in deg.

arising from the metal d subshell belongs mainly to the metal core; therefore, the presence of a V(M) basin accounts for the presence of an s-type electron. The initial MNH_3^+ complex is characterized by the presence of two core basins, C(M) and C(N), and four valence basins, in the case of the low-spin-state isomers, i.e., one V(M, N) that accounts for the metal−nitrogen valence bond and three V(N, H) corresponding to the N−H covalent bonds. As has been previously mentioned, in the case of the high-spin state complexes, there is, in addition, a monosynaptic V(M) basin. In all cases, the population of this basin is found to be around 0.65 electrons. The V(M, N) electron basin populations fall in the range of 1.70−2.00 electrons depending on the complex, and in all cases, the main contribution to this electron basin population comes almost 90% from nitrogen, which indicates the presence of a dative covalent bond.

Continuing on the reaction path to the first transition state, TS1, it has been found that in all cases this structure is characterized by the presence of a V(M, H) basin, with a population of around 1.60 electrons, which means that a weak M−H bond is already formed. For the species in a high-spin state, this formation implies the vanishing of the V(M) basin, together with the breaking of one of the N−H covalent bonds. At the same time, it is verified that there is an important increase of the V(N, M) electron basin population, which, for all the TS1's, falls in a range between 2.50 electrons (for Cu TS1) and 2.80 electrons (for the Ni doublet spin state). Therefore, the first transition state belongs to a different stability domain[34] with respect to the first metal−ligand complex, because a change in the number (and type) of basins has been verified. In the next step, the formation of the first reaction intermediate, $HMNH_2^+$, involves no topological changes, but only small charge transfers between the basins. An increment of the V(M, H) basin population indicates an increase of the strength of the M−H covalent bond, with the only exception being the Cu intermediate, for which the population of that basin is still quite low, i.e., 1.55 electrons.

The transfer of the second hydrogen involves the formation of a second transition state, in which the N−H bond corresponding to the H atom being transferred is still present but very weakened, as well as the M−H formed in the previous step. At the same time, the V(M, N) basin populations are remarkably increased in this transition state, their values being very close to 4 electrons (in all cases), and characterized by the presence of two V(N, M) attractors,

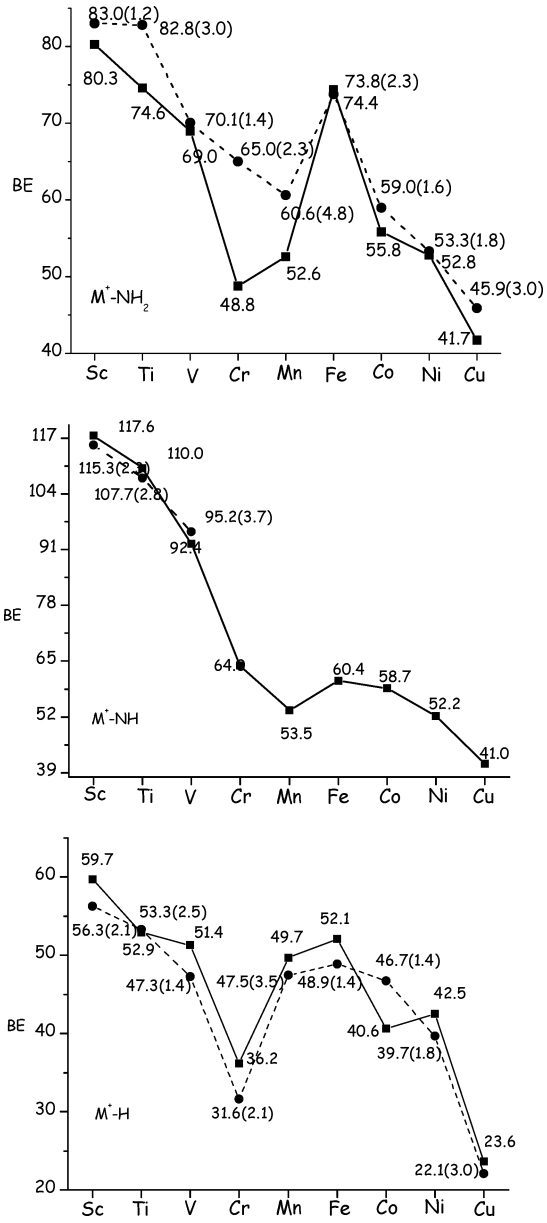

Figure 6. Results from this work versus experimental data in the literature (refs 12−14 and 43−50) for 0 K binding energies in kcal/mol of first-row transition metal ion systems MNH_2^+, MNH^+, and MH^+.

which indicate that a double bond exists between the metal and the N atom of these species.

From a topological point of view, the second reaction intermediate is characterized by the presence of a disynaptic V(H, H) valence basin, and the populations of the rest of the basins, which are very close to those of the reaction product MNH^+, indicate that in this intermediate the H_2 molecule is already structurally prepared for the detachment.

3.4. Periodic Trends. Gas-phase metal−ligand bond strength determination has become the subject of a lot of experimental and theoretical work in recent years. This interest is motivated by the importance that the knowledge of this information has, for example, in elucidating the bonding in transition metal systems, in understanding the mechanism of a variety of catalytic reactions, and in bridging the gap between ion chemistry in the gas phase and in

Table 5. Calculated B3LYP/TZVP[a] and Experimental Binding Energies (BEs) in kcal/mol for the Ground States of MNH^+, MNH_2^+, and MNH^+ Species from Sc^+ to Cu^+

	MH^+				MNH_2^+				MNH^+			
cation	BE	expt[b]	3d[c]	state	BE	expt[b]	3d[c]	state	BE	expt[b]	3d[c]	state
Sc	59.7	56.3 ± 2.1	0.75	$^2\Delta$	80.3	83.0 ± 1.2	1.25	$^2A_1$	117.6	115.3 ± 2.3	1.23	$^1\Sigma^+$
Ti	52.9	53.3 ± 2.5	2.43	$^3\Phi$	74.6	82.8 ± 3.0	2.49	$^3A_1$	110.0	107.7 ± 2.8	2.44	$^2\Delta$
V	51.4	47.3 ± 1.4	3.48	$^4\Delta$	69.0	70.1 ± 1.4	3.37	$^4A_1$	92.4	95.2 ± 3.7	3.48	$^3\Sigma^+$
Cr	36.2	31.6 ± 2.1	4.59	$^5\Sigma^+$	48.8	65.0 ± 2.3	4.57	$^5A_1$	64.0		4.29	$^4\Sigma^+$
Mn	49.7	47.5 ± 3.5	5.23	$^6\Sigma^+$	52.6	60.6 ± 4.8	5.35	$^6A'$	53.5		5.34	$^5A''$
Fe	52.1	48.9 ± 1.4	6.22	$^5\Delta$	74.4	73.8 ± 2.3	6.36	$^5A_1$	60.4		6.35	$^6\Sigma^+$
Co	40.6	46.7 ± 1.4	7.44	$^4\Phi$	55.8	59.0 ± 1.6	7.58	$^4A_1$	58.7		7.65	$^5\Delta$
Ni	42.5	39.7 ± 1.8	8.46	$^3\Delta$	52.8	53.3 ± 1.8	8.69	$^3A'$	52.2		8.78	$^4A''$
Cu	23.6	22.1 ± 3.0	9.65	$^2\Sigma^+$	41.7	45.9 ± 3.0	9.78	$^2A_1$	41.0		9.77	$^3A''$

[a] The basis sets refer to the metal atom. [b] Experimental values are taken from refs 12−14, 43−50. [c] Natural population analysis (ref 51).

solution. In this perspective, a useful strategy is to analyze the trends in metal−ligand binding energies resulting from the variation of the transition metal center, the ligand, and the number of ligands.

In this context, we present a comparison of bond energies, collected in the present and from our previous work on this subject, of some of the fragments arising from the interaction of the first-row transition cation with ammonia. The examined systems are the ground states of MH^+, MNH_2^+, and MNH^+ for the cations in the row from Sc to Cu. Geometrical parameters for these fragments are collected in Table 4. The calculated binding energies are presented graphically in Figure 6 together with available experimental values,[12−14,43−50] whereas in Table 5 we also specify the electronic state and the metal 3d population[51] of each species. All the reported values are of B3LYP/TZVP quality except for those species involving the iron cation. Indeed, for iron, a newly developed DZVP basis set has been employed, which solves the well-known problems met by DFT in the description of atomic ground states.[15d]

Several observations are noteworthy. The calculated bond strength in hydride cations decreases from Sc to Cr, increases for Mn and Fe, and then decreases until Cu, with the binding energy for Co cation slightly lower than that for Ni^+, in contrast with the experimental findings. Because the σ bond is formed through a spin pair of the 1s H orbital and the 4s orbital of the metal in its $4s3d^{n-1}$ configuration, the observed trend is the result of a balance between the loss of exchange energy and the required promotion energy. For example, the particularly stable d^5 and d^{10} configurations for Cr^+ and Cu^+, respectively, are responsible for the low bond energies of CrH^+ and CuH^+ species, whereas the spin pairing causes, for the sd^5 ground state configuration of Mn, a sensible loss of exchange energy which leads to a weakening of the bond. Analogous conclusions have been drawn by other authors.[52,53]

Similar arguments can be used to justify the trend of binding energies for metal−imido and −amide complexes going from Sc to Cu. The metal−imido complexes of the early metals of the series have rather large binding energies, which can be explained in terms of the multiple bond character between the metal and the NH moiety. For the first three metals of the series, a strong triple bond is formed including a dative interaction of the nitrogen lone pair with the accessible d orbitals of the metal. A difference exists in the case of vanadium, for which a promotion to the $4s3d^{n-1}$ excited configuration is necessary in order to form a covalent bond by spin pairing of the V 4s orbital and the N sp orbital. The chromium cation's stable half-filled d^5 configuration is lost because of the necessity to promote one electron into an s orbital, by which is formed one of the three covalent bonds that characterize this system. The net result is a weakening of the bond. The manganese complex shows a smaller binding energy according to the presence of a single bond formed through a spin pair of the 4s orbital of the metal and one sp^2 hybridized nitrogen orbital of the NH group, the bent geometry[15c] allowing accommodation of the lone pair. Linear structures characterize the high-spin iron and cobalt complexes, which are formed by means of the dative interaction of the nitrogen lone pair with empty 4s orbitals of the metal. The nitrogen atom of the $NiNH^+$ complex is calculated to be sp^2 hybridized (see Table 4), and a covalent bond is formed by the 4s orbital of the metal, in its excited configuration, and one unpaired electron of the NH group. The formation of a dative bond through the donation of the nitrogen lone pair into the s orbital allows Cu^+ to retain its stable d^{10} configuration.

The bond energies of amide ions (MNH_2^+) of early metals are consistent with the interpretation that the NH_2 group is doubly bonded to the metal, the additional bond arising from the dative interaction of the nitrogen lone pair with empty metal 3d orbitals. For vanadium and chromium, spin pairing is obtained at the expense of promotion to the $4s3d^{n-1}$ excited configuration. The reduced bond strength for the amide complex of manganese, lacking in empty d orbitals, is attributed to the absence of the dative bond. A sudden increase of the binding energy for iron is due to a double bond formation, which follows the promotion to the excited d^7 configuration. The presence of a single bond characterizes

(43) Elkind, J. L.; Sunderlin, S. L.; Armentrout, P. B. *J. Phys. Chem.* **1989**, *93*, 3151.
(44) Elkind, J. L.; Armentrout, P. B. *Int. J. Mass Spectrom. Ion Processes* **1988**, *83*, 259.
(45) Elkind, J. L.; Armentrout, P. B. *J. Phys. Chem.* **1985**, *89*, 5626.
(46) Elkind, J. L.; Armentrout, P. B. *J. Chem. Phys.* **1987**, *86*, 1868.
(47) Chen, Y.; Armentrout, P. B. *J. Phys. Chem.* **1995**, *99*, 10775.
(48) Elkind, J. L.; Armentrout, P. B. *J. Chem. Phys.* **1986**, *84*, 4862.
(49) Elkind, J. L.; Armentrout, P. B. *J. Am. Chem. Soc.* **1986**, *108*, 2765.
(50) Elkind, J. L.; Armentrout, P. B. *J. Phys. Chem.* **1986**, *90*, 6576.
(51) Glendening, E. D.; Reed, A. E.; Carpenter, J. E.; Weinhold, F. *NBO*, version 3.1.
(52) Schilling, J. B.; Goddard, W. A., III; Beauchamp, J. L. *J. Am. Chem. Soc.* **1986**, *108*, 582.
(53) Elkind, J. L.; Armentrout, P. B. *J. Phys. Chem.* **1987**, *91*, 2037.

the structures of the complexes of the remaining cations (Co−Cu). In all cases, the bond is formed through a dative interaction between the nitrogen lone pair and the empty 4s orbital of the metals in their ground state configurations. As can be realized from the metal d population reported in Table 5, NBO analysis confirms that in most of the cases the bonding is derived from a mixture of the $4s3d^{n-1}$ and $3d^n$ metal configurations.

The behaviors along the PES's for the insertion reaction into the N−H bond in going from scandium to copper cations can be rationalized by taking into account the stability trends of intermediates and fragments obtained from the three examined exit channels. The reaction is exothermic, with energy barriers of transition states below the dissociation limit, only for scandium and titanium. The stability of the insertion intermediate (**I**) decreases from left to right with a minimum corresponding to chromium, as a result of the promotion to an electronic configuration suitable for the formation of two σ bonds. As a consequence of the spin pairing, the loss of exchange energy for some elements further contributes to the decreased stability. The energetics of the formation of the second hydrogen−molecule complex (**II**) and of the final products is in line with the binding energies of the fragments examined here.

4. Conclusions

The PES's for the reactions of late first-row transition metal cations (Co^+, Ni^+, Cu^+) with ammonia have been computed and analyzed. Both high- and low-spin PES's have been characterized in detail at the B3LYP level of theory. The energy diagrams are uphill in all cases toward formation of dehydrogenation products, and at low kinetic energies, only the exothermic formation of the first ion−dipole complex is possible. Moreover, also at high temperatures, the necessity to overcome high energy barriers makes simple bonds breaking to give MNH_2^+ and MH^+ fragments more likely than insertion intermediate formation and hydrogen elimination from the ligand. The picture of the behaviors along the paths has been supported by a topological description, based on the gradient field analysis of the electron localization function, of all the key minima and transition states along the reaction pathways in order to characterize the bonding. The very reasonable agreement with available experimental data of calculated energetics of exit channels and binding energies supports the reliability of the experimentally unavailable values. A comparison between the results of the present work for late first-row transition metals and those for early and middle first-row transition metals is given.

Acknowledgment. Financial support from the Università degli Studi della Calabria and MIUR is gratefully acknowledged.

IC049696D